Supporting Information

Data-Driven Discovery of Novel Chalcogenide Semiconductors for Solar Absorption

Md Habibur Rahman, Arun Mannodi-Kanakkithodi*

School of Materials Engineering, Purdue University, West Lafayette, IN 47907, USA

*Corresponding author: amannodi@purdue.edu

Construction of the A_2BCX_4 and ABX_2 Chemical Spaces

For the A_2BCX_4 series, we considered 6 possible A cations, 6 B cations, 3 C cations, and 3 X anions. Fractional occupancies were permitted as follows: A = {0, 0.5, 1, 1.5, 2}, B = {0, 0.5, 1}, C = {0, 0.5, 1}, and X = {0, 1, 2, 3, 4}. E.g., the 6 possible monovalent cations at the A-site (Na, K, Rb, Cs, Cu, and Ag) could each adopt one of any of the fractional occupancies {0, 0.5, 1, 1.5, 2} such that the total sums to 2; analogous rules hold for every other site. Denoting these occupancies by $\{a_1, a_2, a_3, a_4, a_5, a_6\}$, non-negative solutions are sought for the equation:

$$a_1 + a_2 + a_3 + a_4 + a_5 + a_6 \;=\; 2, \quad a_i \in \{0,\, 0.5,\, 1,\, 1.5,\, 2\}.$$

The number of solutions is given by:

$$\binom{4+6-1}{6-1} \;=\; \binom{9}{5} \;=\; 126.$$

For the B, C, and X sites (list of all constituent chemical species shown in **Figure S2**), the number of valid solutions were calculated to be 21, 6, and 15, respectively, which ultimately leads to $126 \times 21 \times 6 \times 15 = 238{,}140$ total compositions. Considering two types of nominal cation ordering (not accounting for the additional disorder with alloying) doubles

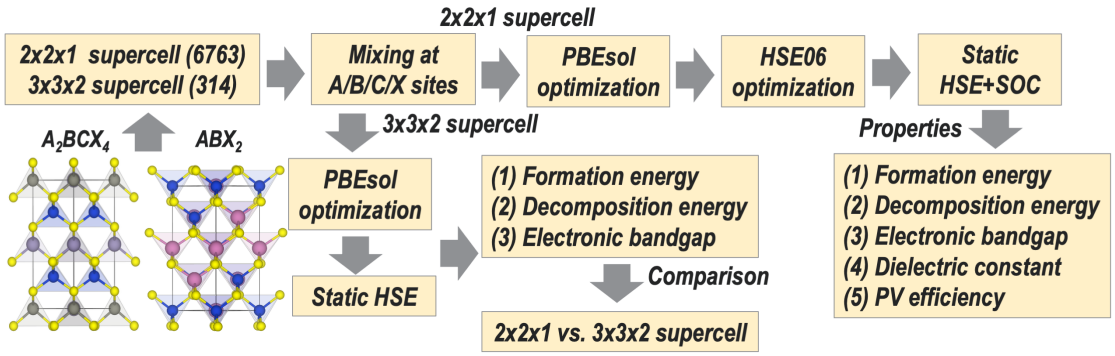

Figure S1: DFT workflow used in this study— targeted mixing at the A, B, C, and X sites was applied to $2 \times 2 \times 1$ and $3 \times 3 \times 2$ supercells, followed by geometry optimization using the PBEsol and HSE06 functionals. Finally, static HSE+SOC calculations were performed on the HSE06-optimized geometry to accurately determine the properties of interest.

this to 476,280. Out of these compounds, there are 648 pure unalloyed compositions, 12,960 compounds with only A-site mixing, 1,620 compounds with only B-site mixing, 648 compounds with only C-site missing, 2,592 compounds with only X-site mixing, and 457,812 total compounds with simultaneous mixing across multiple sites.

Similarly, for the ABX_2 series, we considered 6 possible A cations, 3 B cations, and 3 X anions. To keep it consistent with the definitions for the A_2BCX_4 series, fractional occupancies were allowed as: $A = \{0, 0.25, 0.5, 0.75, 1\}$, $B = \{0, 0.25, 0.5, 0.75, 1\}$, $X = \{0, 0.5, 1, 1.5, 2\}$. This leads to a total of 126, 15, and 15 possibilities for A-site mixing, B-site mixing, and X-site mixing, respectively, resulting in $126 \times 15 \times 15 = 28{,}350$ unique compositions. Considering two types of nominal cation ordering again, this number doubles to 56,700. Among these 56,700 compositions, 108 are pure compounds, 2,160 involve only A-site mixing, 432 involve only B-site mixing, 432 involve only X-site mixing, and 53,568 involve simultaneous multi-site mixing.

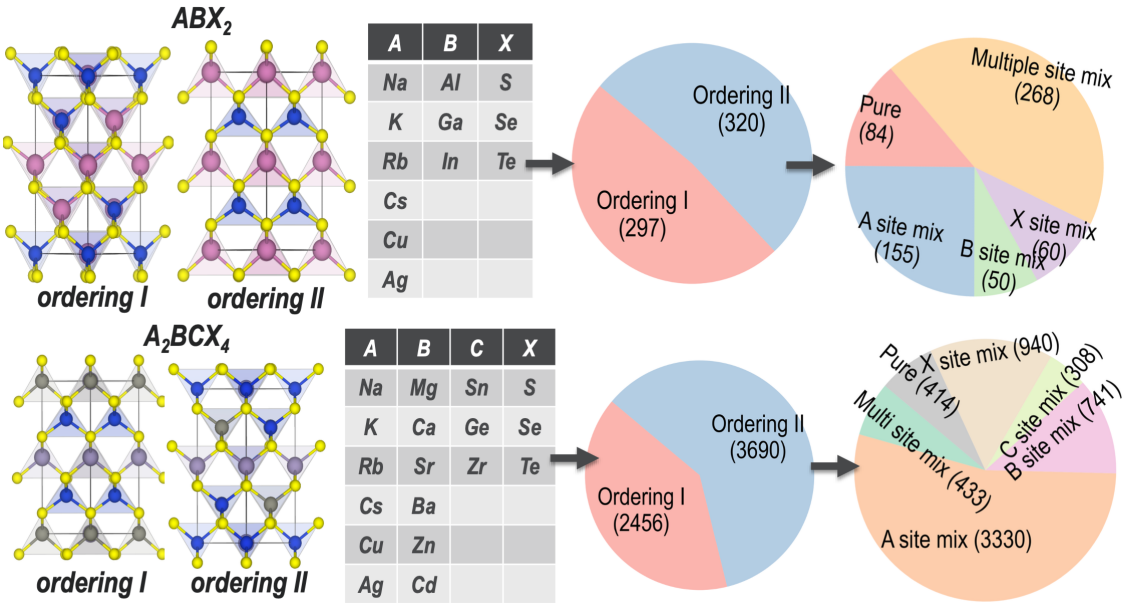

Figure S2: Construction of the ABX_2 and A_2BCX_4 datasets. (Left) Crystal prototypes considered. (Middle) Elemental space explored for A, B, C, and X sites. (Right) Distribution of generated compounds across structural orderings (ordering I vs ordering II for ABX_2; ordering I vs ordering II for A_2BCX_4) and across composition types (pure, single-site mixing, and multiple-site mixing). The total number of structures in each category is indicated in parentheses.

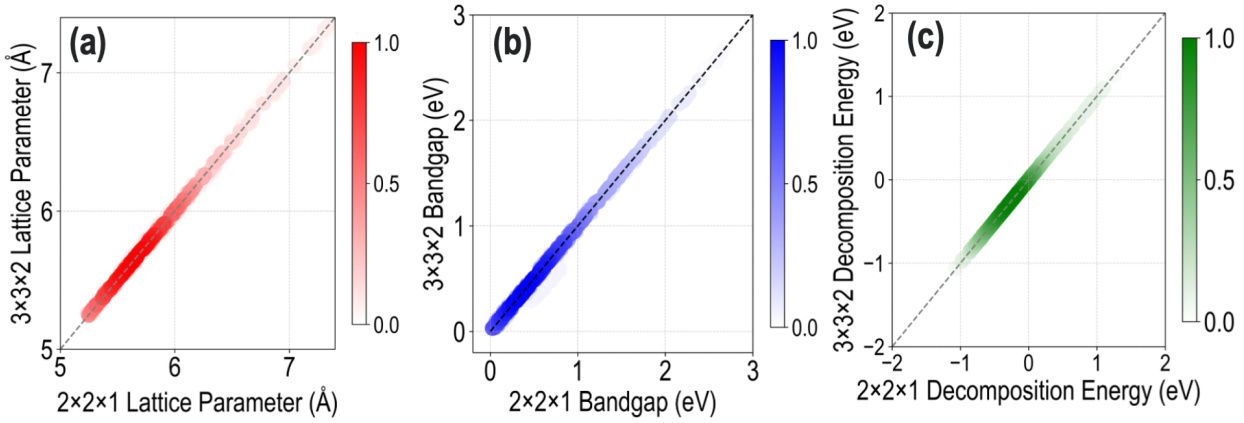

Figure S3: Comparison of DFT-computed (PBEsol) properties from $2 \times 2 \times 1$ vs. $3 \times 3 \times 2$: (a) lattice constant, (b) decomposition energy, and (c) bandgap in terms of different cation ordering. The color bar indicates the point density (normalized from 0 to 1), where darker colors represent regions with a higher number of overlapping data points, and lighter colors indicate sparse or less populated regions in the property space.

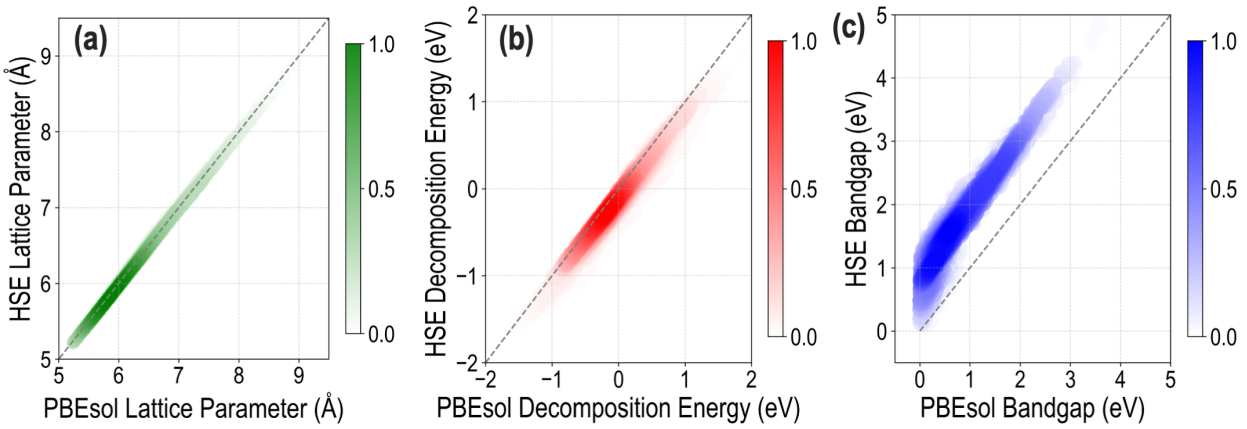

Figure S4: Comparison of DFT-computed properties from PBEsol and HSE06: (a) lattice constant, (b) decomposition energy, and (c) bandgap in terms of different cation ordering. The color bar indicates the point density (normalized from 0 to 1), where darker colors represent regions with a higher number of overlapping data points, and lighter colors indicate sparse or less populated regions in the property space.

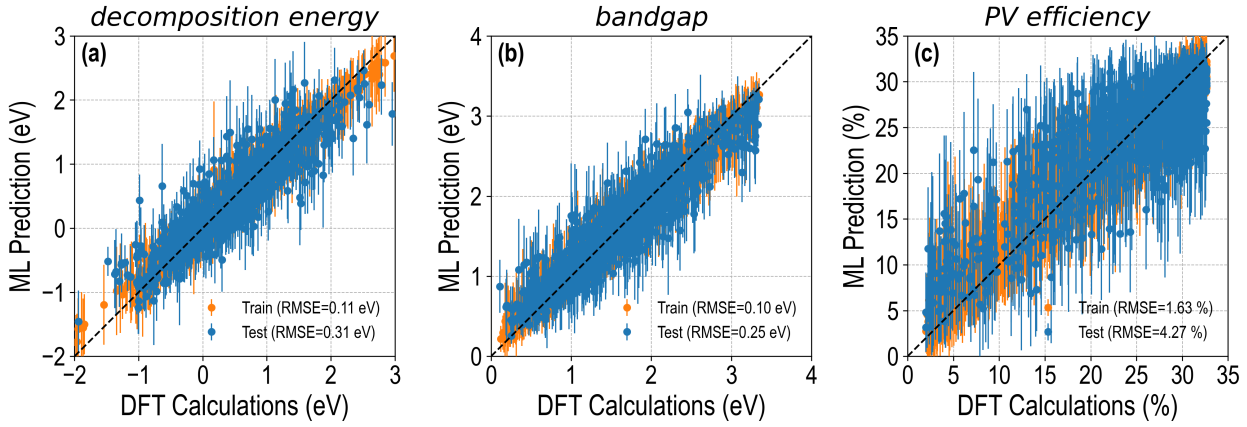

Figure S5: Parity plots for rigorously optimized random forest models for (a) decomposition energy, (b) bandgap, and (c) photovoltaic (PV) efficiency (SLME). The random forest models were trained on an initial dataset of 1,650 compounds with properties computed using the HSE+SOC functional. Error bars represent the standard deviation along with the minimum and maximum values obtained across 50 independently trained random forest models initialized with different random seeds.

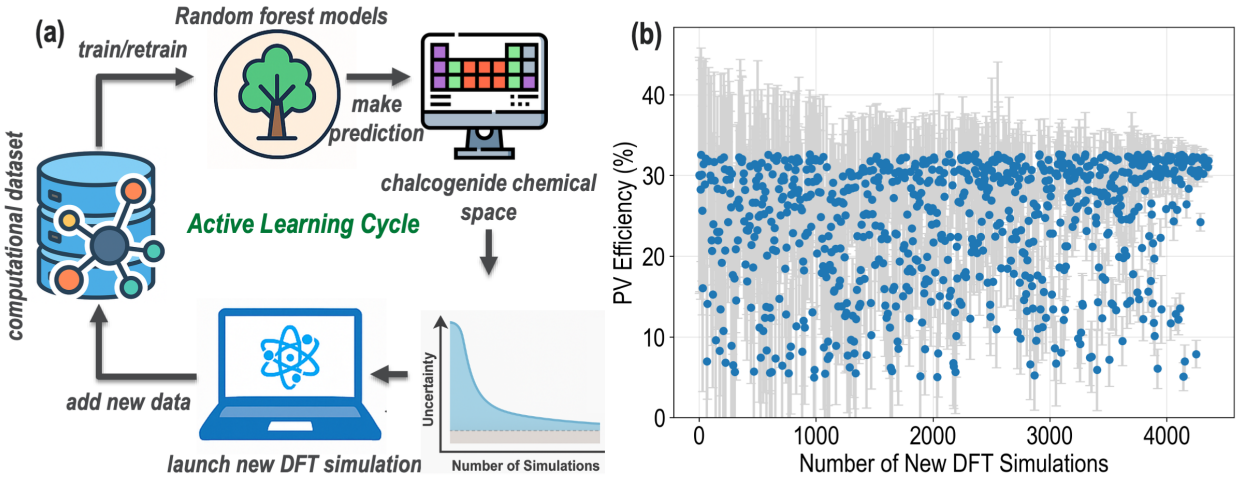

Figure S6: (a) Active learning (AL) workflow used in this study: photovoltaic (PV) efficiency across the remaining design space is initially predicted using a random forest model trained on only 1650 data points. An acquisition function is then employed to identify the most promising candidates for the next round of DFT data to be revealed. The random forest model is iteratively retrained with the newly acquired data and applied to the unexplored design space. (b) AL schedule illustrating the subsequent simulation batches selected via the acquisition function to improve the model and reduce the uncertainties.

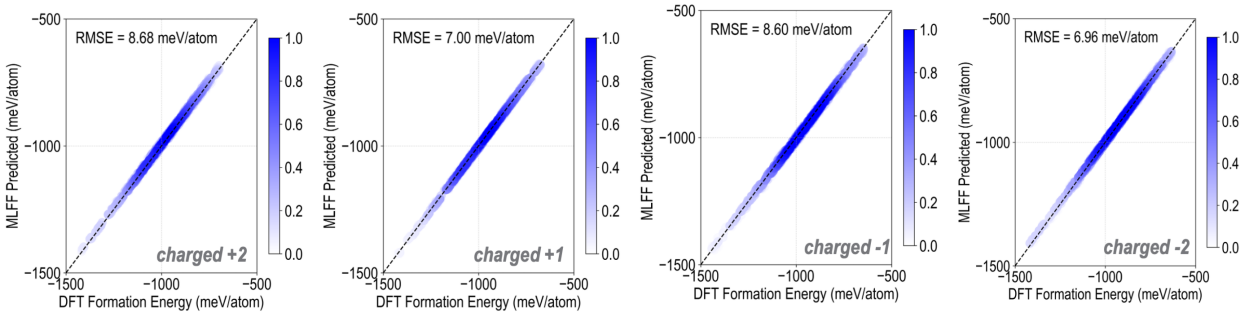

Figure S7: Parity plots comparing DFT crystal formation energies with MLFF-predicted values for four charge states ($q = +2$, $+1$, -1, and -2). The dashed line indicates perfect agreement ($y = x$). The model achieves low prediction errors with RMSE values of 8.68, 7.00, 8.60, and 6.96 meV/atom for $q = +2$, $+1$, -1, and -2, respectively. The color scale denotes the local point density.

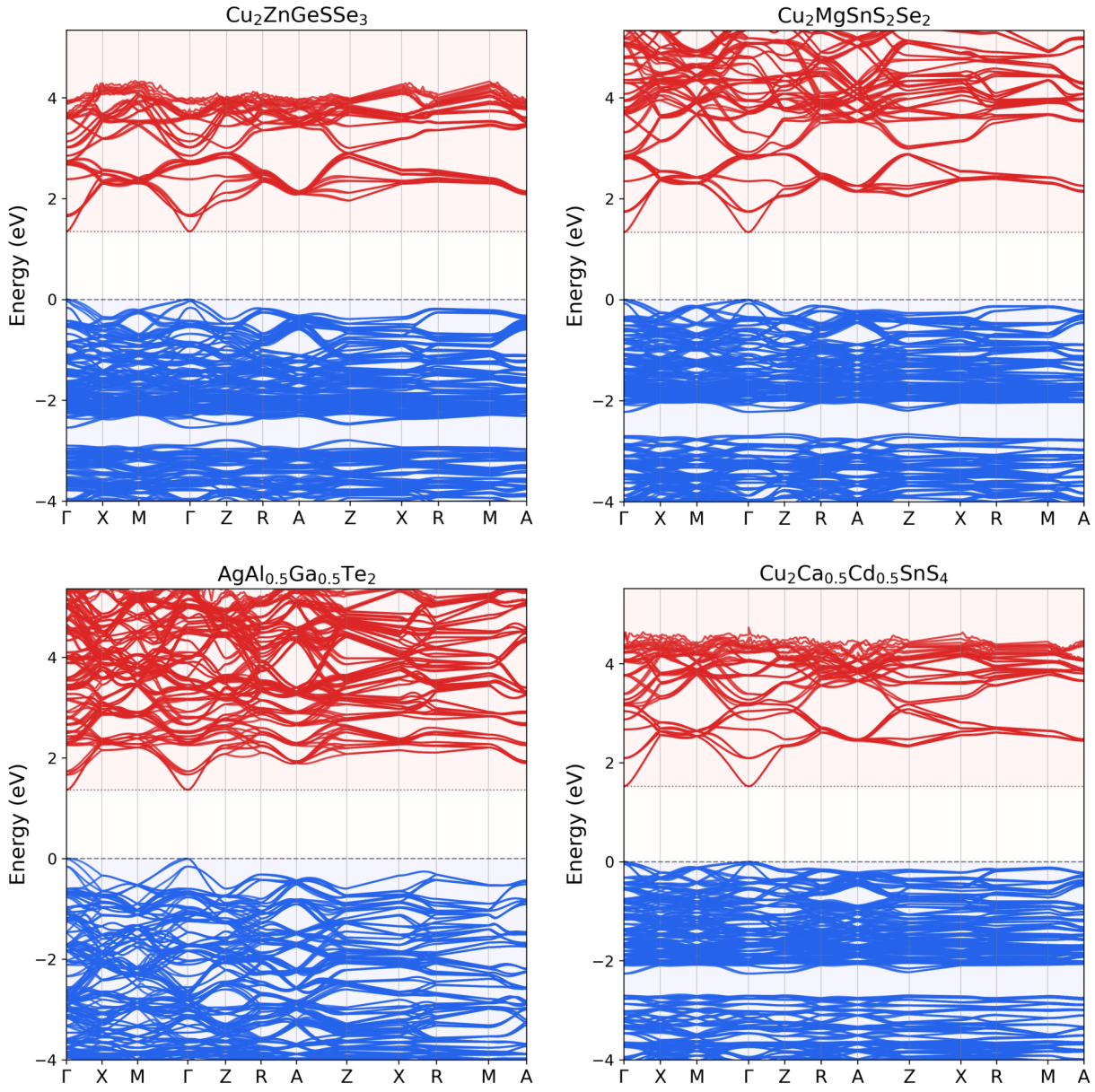

Figure S8: HSE+SOC electronic band structures of four selected top-ranked chalcogenide candidates: (a) $Cu_2ZnGeSSe_3$, (b) $Cu_2MgSnS_2Se_2$, (c) $AgAl_{0.5}Ga_{0.5}Te_2$, and (d) $Cu_2Ca_{0.5}Cd_{0.5}SnS_4$. These compounds span diverse compositions with E_{gap} in the 1.3–1.5 eV range, negative ΔH_{decomp}, and high SLME values. The dispersive band edges suggest moderate effective masses favorable for carrier transport.

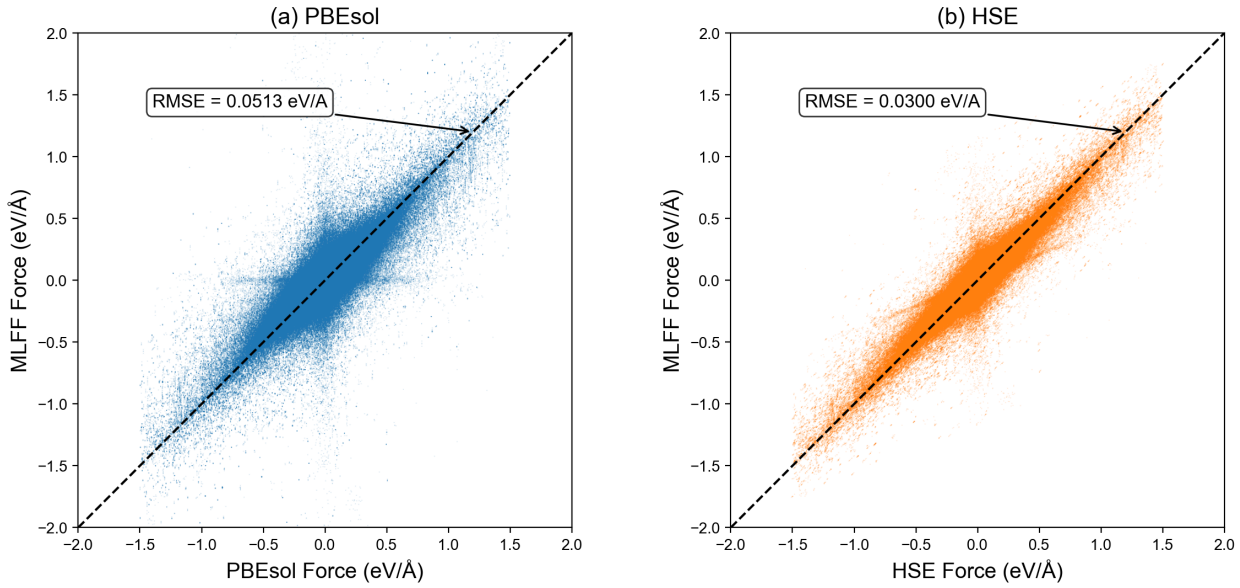

Figure S9: Parity plots of MLFF-predicted vs. DFT forces for neutral defect configurations: (a) PBEsol-trained MLFF (RMSE = 0.051 eV/Å) and (b) HSE-trained MLFF (RMSE = 0.030 eV/Å). The HSE-trained model shows tighter correlation and lower RMSE, confirming that training on HSE data yields more accurate force predictions for defect geometry optimization.

Table S1: Summary of key DFT input parameters used in this work.

Parameter	$2 \times 2 \times 1$ **Supercell**	$3 \times 3 \times 2$ **Supercell**
Atoms per supercell	64	288
ENCUT (eV)	500	500
k-grid (PBEsol relax)	$a_i \times k_i \geq 30$ Å	Γ-only
k-grid (HSE06 relax)	$a_i \times k_i \geq 20$ Å	Γ-only
k-grid (HSE06+SOC static)	$a_i \times k_i \geq 30$ Å	Γ-only
EDIFF (eV)	10^{-5}	10^{-5}
EDIFFG (eV/Å)	-0.01	static
HSE06 mixing (α)	0.25	0.25
HSE06 screening (ω)	0.2 Å^{-1}	0.2 Å^{-1}
PAW pseudopotentials	VASP 6.4.1 recommended	VASP 6.4.1 recommended
Smearing	Gaussian, 0.05 eV	Gaussian, 0.05 eV

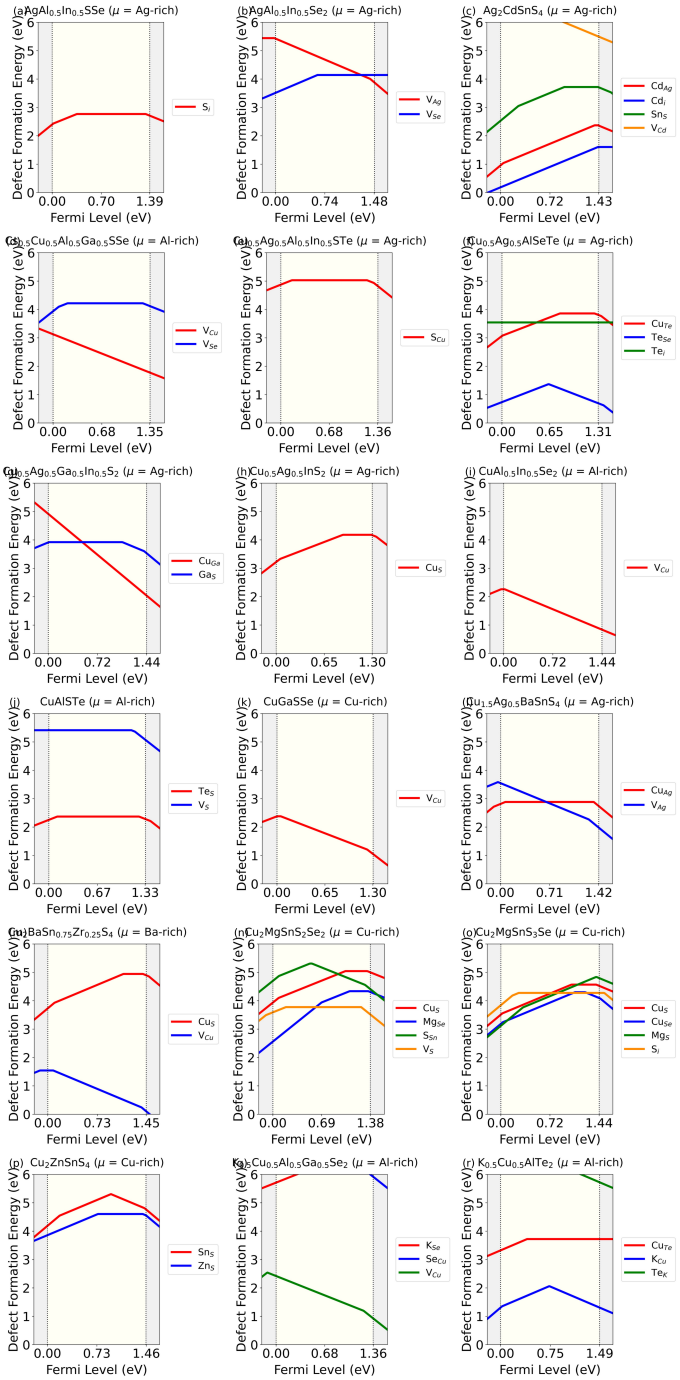

Figure S10: Defect formation energy diagrams under cation-rich chemical potential conditions for 18 representative compounds randomly selected from the 314-compound subset. Calculations were performed using $3 \times 3 \times 2$ supercells (288 atoms) with full PBEsol geometry optimization followed by static HSE06 calculations, in five distinct charge states ($q = +2$ to -2). The selected compounds span Cu-, Ag-, K-, and Cs-containing systems with S, Se, Te, and mixed-anion chemistries. Dashed vertical lines indicate the VBM and CBM (conduction band minimum). The shaded regions outside the E_{gap} are shown in gray.

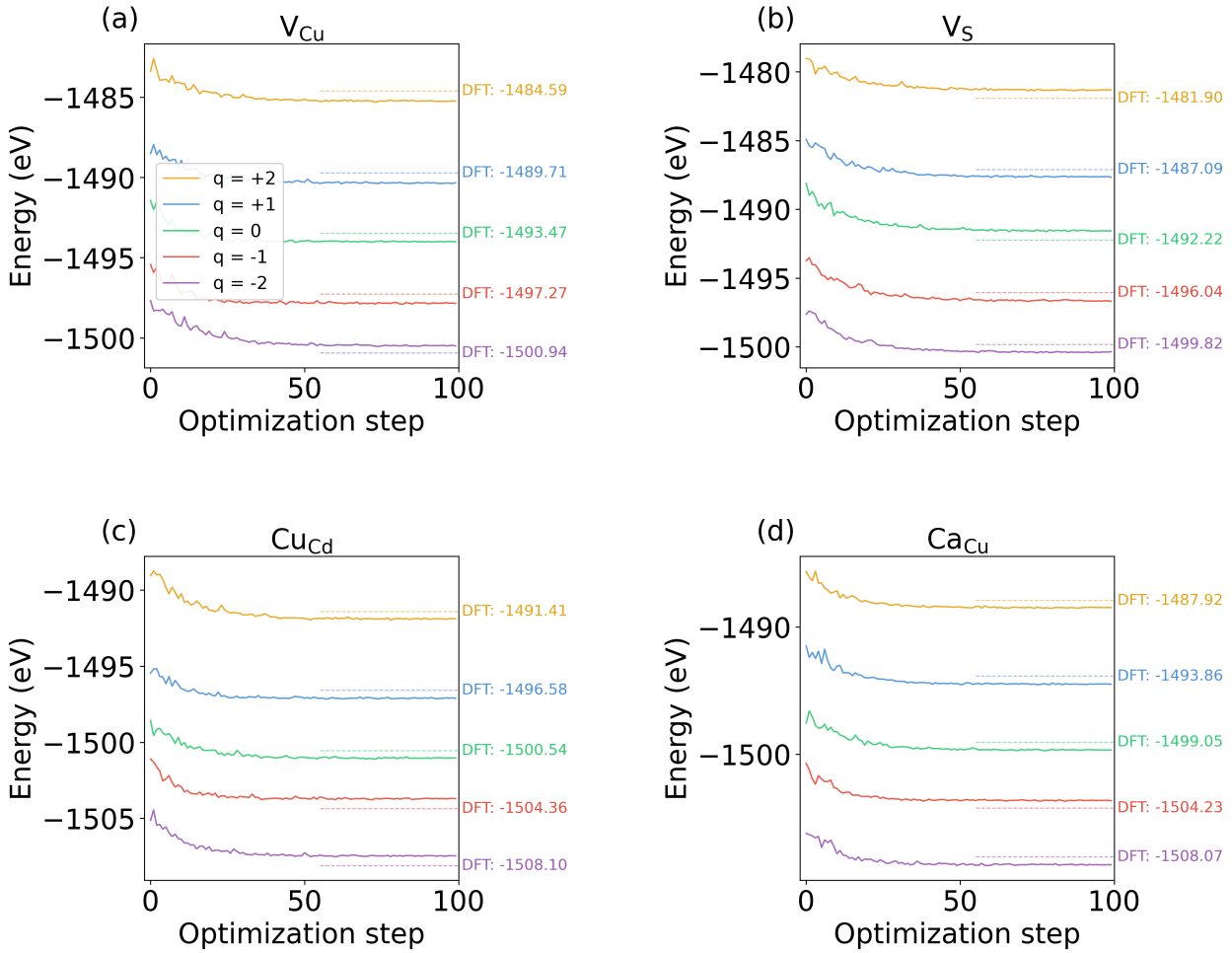

Figure S11: MLFF optimization convergence for four representative defects in $Cu_2Ca_{0.5}Cd_{0.5}SnS_4$ across all five charge states ($q = +2, +1, 0, -1, -2$): (a) V_{Cu}, (b) V_S, (c) Cu_{Cd}, and (d) Ca_{Cu}. Solid lines show the MLFF energy during geometry optimization and dashed lines indicate the corresponding DFT total energies. The MLFF-relaxed energies converge to within $\sim$ 0.5–0.7 eV of the DFT reference values, with no systematic overestimation or underestimation across charge states.

Table S2: Structural comparison between PBEsol and HSE relaxed geometries for $Ag_1Al_{0.5}Ga_{0.5}S_2$.

Property	HSE	PBEsol
Lattice parameters		
a (Å)	5.63	5.62
c (Å)	10.43	10.41
Bond lengths (mean, Å)		
Al–S	2.25	2.23
Ga–S	2.26	2.25
Ag–S	2.51	2.48

Computational Definitions of Formation and Decomposition Energies

Energy normalization

The total energy E_{tot} is obtained from DFT. If the supercell contains N_{sc} atoms and one formula unit contains N_{fu} atoms, then the energy per formula unit is

$$E_{pfu} = \frac{E_{tot}}{N_{sc}} \times N_{fu}.$$

Formation energy

The formation energy is computed as the difference between the compound energy and the sum of the reference elemental energies, divided by the number of atoms in the formula unit. For $Ag_2Ca_{0.5}Sr_{0.5}Sn_{0.5}Ge_{0.5}S_2Te_2$:

$$\Delta H_{form} = \frac{1}{8}\Big[E(Ag_2Ca_{0.5}Sr_{0.5}Sn_{0.5}Ge_{0.5}S_2Te_2) - 2E(Ag) - 0.5E(Ca) - 0.5E(Sr) - 0.5E(Sn) - 0.5E(Ge) - 2E(S) - 2E(Te)\Big]. \quad \text{(S1)}$$

Here the denominator (8) is the total number of atoms per formula unit.

Decomposition energy for A_2BCX_4 compounds

Decomposition is evaluated relative to the most likely set of binary competing phases: - A–X binaries of type A_2X, - B–X binaries of type BX, - C–X binaries of type CX_2. The weights for each binary are determined from stoichiometry: - For the A–X channel, the weight is $(n_A/2) \times (n_X/4)$, where n_A and n_X are the counts of A and X atoms in the formula. - For the B–X channel, the weight is $(n_B/1) \times (n_X/4)$. - For the C–X channel, the weight is $(n_C/1) \times (n_X/4)$. The total competing energy is the sum of all binary references multiplied

by their weights. The decomposition enthalpy is then

$$\Delta H_{decomp} = E_{pfu} - S,$$

where S is the weighted sum of binary reference energies.

Worked example: $Ag_2Ca_{0.5}Sr_{0.5}Sn_{0.5}Ge_{0.5}S_2Te_2$

For this composition: - $A = Ag$ (2 atoms), $B = Ca, Sr$ (0.5 each), $C = Sn, Ge$ (0.5 each), $X = S, Te$ (2 each). Weights are: - Ag_2S and Ag_2Te: each weight $= (2/2) \times (2/4) = 0.5$. - $CaS, CaTe, SrS, SrTe$: each weight $= (0.5/1) \times (2/4) = 0.25$. - $SnS_2, SnTe_2, GeS_2, GeTe_2$: each weight $= (0.5/1) \times (2/4) = 0.25$. Thus the competing energy is

$$\begin{aligned} S = {} & 0.5\big(E(Ag_2S) + E(Ag_2Te)\big) \\ & + 0.25\big(E(CaS) + E(CaTe) + E(SrS) + E(SrTe)\big) \\ & + 0.25\big(E(SnS_2) + E(SnTe_2) + E(GeS_2) + E(GeTe_2)\big). \end{aligned} \tag{S2}$$

The decomposition enthalpy is

$$\Delta H_{decomp} = E(Ag_2Ca_{0.5}Sr_{0.5}Sn_{0.5}Ge_{0.5}S_2Te_2) - S.$$

To account for mixing, a configurational entropy correction is added:

$$\Delta G_{mix} = k_B T \sum_j f_j \ln f_j,$$

where f_j are the mixing fractions for each binary. For this compound: Two channels with fraction 0.5 (Ag–S and Ag–Te) and Eight channels with fraction 0.25 (Ca/Sr with S/Te,

Sn/Ge with S/Te). So:

$$\Delta G_{mix} = k_B T \left[2 \cdot (0.5 \ln 0.5) + 8 \cdot (0.25 \ln 0.25) \right] = -5 k_B T \ln 2.$$

The full decomposition energy is

$$E_{decomp} = \Delta H_{decomp} + \Delta G_{mix}.$$

Negative E_{decomp} means the compound is stable against decomposition into the chosen binaries whereas Positive E_{decomp} means the compound tends to decompose.

List of Defects Considered for Each Compound

The following table summarizes, for each compound, the list of defects considered in our calculations. While detailed defect formation energy diagrams are presented for selected case studies for the sake of brevity, the entire defect dataset spans over 1,000 native point defect configurations across 314 compounds, each computed using a $3 \times 3 \times 2$ supercell with PBEsol geometry optimization followed by static HSE06 calculations. Representative defect formation energy diagrams for 18 randomly selected compounds under cation-rich chemical potential conditions are provided in **Figure S10**. General trends include: (i) Cu/Ag vacancies are consistently the lowest-energy acceptors, supporting p-type conductivity; (ii) anion-related defect energetics are sensitive to the anion species, with Te-containing compounds showing higher formation energy defects; (iii) anti-site defects involving B/C-site cations most frequently introduce deep levels in the E_{gap}; and (iv) several compounds exhibit high minimum defect formation energies (> 3 eV) across the entire E_{gap}, indicating strong defect tolerance.

Table S3: List of native point defects considered for each compound, organized by composition and cation ordering. Defect calculations were performed in $3 \times 3 \times 2$ supercells using PBEsol geometry optimization followed by static HSE06 electronic structure calculations in five charge states ($q = +2, +1, 0, -1, -2$).

Compound	**Ordering**	**Defects Considered**
$AgAl_{0.5}Ga_{0.5}S_2$	Ordering I	V_S, V_{Al}
$AgAl_{0.5}Ga_{0.5}Se_2$	Ordering I	Ag_{Se}, V_{Al}, Se_{Al}
$AgAl_{0.5}Ga_{0.5}Se_2$	Ordering II	Ag_{Ga}, V_{Ag}, Ga_i, Ga_{Ag}
$AgAl_{0.5}Ga_{0.5}Te_2$	Ordering II	Al_{Ga}, Ag_{Ga}, V_{Te}, Ga_{Al}
$AgAl_{0.5}In_{0.5}SSe$	Ordering I	Se_S, S_{Ag}, Al_{In}, Ag_{Al}, In_{Al}, V_{Al}, In_S
$AgAl_{0.5}In_{0.5}SSe$	Ordering II	S_i, Al_S, Se_S
$AgAl_{0.5}In_{0.5}S_2$	Ordering I	V_{Al}, In_{Al}
$AgAl_{0.5}In_{0.5}Se_2$	Ordering I	In_{Al}, V_{Al}, V_{Se}, V_{Ag}, Al_{Se}
$AgAl_{0.5}In_{0.5}Se_2$	Ordering II	Ag_i, Al_i, V_{Se}
$AgAl_{0.5}In_{0.5}Te_2$	Ordering II	V_{Al}
AgAlSSe	Ordering I	Se_S, V_{Se}, Ag_S, Se_{Ag}
$AgAlS_2$	Ordering I	V_S, Al_S
$AgAlS_2$	Ordering II	V_S, Al_S
$AgAlSe_2$	Ordering I	V_{Se}, Al_i
$AgAlSe_2$	Ordering II	Ag_{Se}, Al_{Ag}, Al_{Se}
$AgAlTe_2$	Ordering I	Te_{Ag}, Al_i, Ag_{Al}
$AgAlTe_2$	Ordering II	V_{Ag}

Continued on next page

Table S3 – continued from previous page

Compound	**Ordering**	**Defects Considered**
$AgGa_{0.5}In_{0.5}S_2$	Ordering I	Ag_i, Ag_{In}, S_{In}
$AgGa_{0.5}In_{0.5}S_2$	Ordering II	In_{Ga}
$AgGa_{0.5}In_{0.5}Se_2$	Ordering I	Ag_i, V_{Ag}
$AgGa_{0.5}In_{0.5}Se_2$	Ordering II	V_{Ga}
AgGaSTe	Ordering I	Te_{Ga}, Ag_{Te}
AgGaSTe	Ordering II	Ga_i, Ag_i, Te_{Ga}, V_{Ag}
$AgGaS_2$	Ordering I	V_S, Ag_{Ga}, Ga_i
$AgGaS_2$	Ordering II	Ga_{Ag}, Ag_S
AgGaSeTe	Ordering II	Ag_{Ga}, Ga_{Te}, Te_{Ga}
$AgGaSe_2$	Ordering I	Ag_{Se}
$AgGaSe_2$	Ordering II	V_{Ga}, Ga_{Se}, Ag_{Se}
AgInSSe	Ordering I	Ag_i, S_{In}, In_{Ag}, Ag_{Se}
AgInSSe	Ordering II	V_{Ag}
$AgInSe_2$	Ordering I	Se_{Ag}
$AgInSe_2$	Ordering II	V_{Ag}
$Ag_2BaGeSe_4$	Ordering II	Ag_{Ge}, V_{Ba}, V_{Ge}
Ag_2BaSnS_4	Ordering I	Ag_{Sn}
Ag_2BaSnS_4	Ordering II	Sn_{Ba}, V_{Sn}, V_S
$Ag_2Ca_{0.5}Cd_{0.5}ZrSe_4$	Ordering I	Zr_{Ca}, Cd_i, V_{Cd}, Zr_i, Zr_{Cd}, Cd_{Ag}

Continued on next page

Table S3 – continued from previous page

Compound	**Ordering**	**Defects Considered**
$Ag_2Ca_{0.5}Cd_{0.5}ZrSe_4$	Ordering II	Zr_i, Zr_{Se}, V_{Se}, V_{Cd}, Se_{Ca}, Se_{Zr}
$Ag_2CaGeSSeTe_2$	Ordering I	S_{Ca}, Ag_{Se}, S_{Te}
$Ag_2CaGeSSe_3$	Ordering I	Ca_S, V_{Ag}, Ge_{Se}, Ag_{Ca}
$Ag_2CaGeSSe_3$	Ordering II	Ge_i, Se_{Ge}
Ag_2CaGeS_2SeTe	Ordering I	Ca_{Se}, Ge_{Ag}, Se_{Ag}, Te_i
Ag_2CaGeS_2SeTe	Ordering II	V_S, Se_{Ag}
Ag_2CaGeS_4	Ordering II	Ag_i, Ge_i
$Ag_2CaGeSe_4$	Ordering II	Se_i, Ca_{Se}
Ag_2CaSnS_4	Ordering I	Ag_{Ca}, Sn_{Ca}
Ag_2CaSnS_4	Ordering II	Ca_S, Sn_{Ca}, V_{Sn}, S_{Sn}, Ca_{Sn}, Ca_{Ag}
Ag_2CdGeS_4	Ordering II	V_{Cd}, S_{Ag}, Cd_S, Ge_{Ag}, Ag_{Cd}, S_i
$Ag_2CdGeSe_4$	Ordering I	Se_{Ge}, Cd_{Ag}, V_{Ag}, Se_{Ag}
$Ag_2CdGeSe_4$	Ordering II	Cd_{Ge}, Ge_{Se}, Cd_i, Ag_{Se}, Cd_{Se}
Ag_2CdSnS_4	Ordering I	Sn_S, Cd_{Ag}, Cd_i, S_{Ag}, V_{Cd}
$Ag_2CdSnSe_4$	Ordering I	V_{Cd}, Sn_{Cd}
$Ag_2CdSnSe_4$	Ordering II	Sn_{Ag}, Sn_i
$Ag_2Mg_{0.5}Ba_{0.5}ZrS_4$	Ordering I	V_{Mg}, Zr_{Ba}, Mg_S
$Ag_2Mg_{0.5}Ba_{0.5}ZrS_4$	Ordering II	Mg_S, S_i, Ag_S, V_S, S_{Zr}, Ag_{Ba}
Ag_2MgGeS_4	Ordering I	Mg_S

Continued on next page

Table S3 – continued from previous page

Compound	**Ordering**	**Defects Considered**
Ag_2MgGeS_4	Ordering II	S_i, S_{Ag}
$Ag_2MgGeSe_4$	Ordering I	Mg_{Ge}, Se_{Ge}, Mg_{Se}
$Ag_2MgGeSe_4$	Ordering II	Ge_{Se}, Mg_{Se}, V_{Ge}
$Ag_2MgGeTe_4$	Ordering I	Ge_{Te}, Ge_i
$Ag_2MgGeTe_4$	Ordering II	Te_{Ag}, Ge_i, Te_{Ge}, Mg_i
Ag_2MgSnS_4	Ordering I	V_{Ag}, Ag_i, S_i, Mg_i
$Ag_2MgSnSe_4$	Ordering I	Ag_{Sn}, Mg_{Ag}, Sn_{Se}
$Ag_2MgSnSe_4$	Ordering II	Sn_{Ag}, Se_{Mg}
$Ag_2MgZrS_2Se_2$	Ordering I	V_{Ag}, S_{Ag}, Ag_{Zr}, S_{Zr}, S_i, Mg_S, Se_{Ag}
$Ag_2MgZrS_2Se_2$	Ordering II	Se_S
Ag_2SrGeS_4	Ordering II	Sr_i, S_{Ge}, V_{Ge}
Ag_2SrSnS_4	Ordering I	V_{Sr}, Sr_S, V_S
$Ag_2SrSnSe_4$	Ordering II	Ag_{Se}, Se_i
Ag_2SrZrS_2SeTe	Ordering II	Zr_{Ag}, Ag_{Sr}, Zr_{Se}, V_S, V_{Se}, Te_{Sr}, Sr_i, S_{Se}, Te_{Ag}, Te_{Zr}, Te_{Se}
Ag_2ZnGeS_4	Ordering I	Ag_{Zn}
Ag_2ZnGeS_4	Ordering II	V_S, Ag_{Zn}
$Ag_2ZnGeSe_4$	Ordering I	Ag_{Zn}, Se_{Zn}
Ag_2ZnSnS_4	Ordering I	Ag_i, Zn_i

Continued on next page

Table S3 – continued from previous page

Compound	**Ordering**	**Defects Considered**
$Ag_2ZnSnSe_4$	Ordering I	Zn_{Se}
$Ag_2ZnSnSe_4$	Ordering II	Se_i
$Cs_{0.5}Ag_{0.5}Al_{0.5}In_{0.5}SSe$	Ordering II	S_{Cs}, V_{Cs}, V_S, V_{Ag}, Al_{Cs}, V_{In}
$Cs_{0.5}Ag_{0.5}Al_{0.5}In_{0.5}S_2$	Ordering I	Al_{Ag}, S_{In}, Cs_{Ag}, Al_i
$Cs_{0.5}Ag_{0.5}AlSSe$	Ordering I	Se_{Al}, V_{Al}, Ag_{Cs}
$Cs_{0.5}Ag_{0.5}AlSeTe$	Ordering I	Al_{Te}, Te_i, Cs_{Se}
$Cs_{0.5}Ag_{0.5}AlSeTe$	Ordering II	Se_{Ag}, Al_{Se}
$Cs_{0.5}Ag_{0.5}AlSe_2$	Ordering I	V_{Al}, Se_i, V_{Ag}
$Cs_{0.5}Ag_{0.5}AlTe_2$	Ordering I	Cs_{Ag}, Al_i, Te_{Cs}
$Cs_{0.5}Ag_{1.5}MgSnSe_4$	Ordering I	Mg_{Cs}, V_{Ag}
$Cs_{0.5}Ag_{1.5}MgSnSe_4$	Ordering II	V_{Se}, Se_{Cs}, Sn_{Cs}, Mg_{Ag}
$Cs_{0.5}Cu_{0.5}Al_{0.5}Ga_{0.5}SSe$	Ordering II	Cu_{Al}, V_{Cu}, V_{Se}, S_{Al}
$Cs_{0.5}Cu_{0.5}Al_{0.5}Ga_{0.5}S_2$	Ordering II	V_{Ga}
$Cs_{0.5}Cu_{0.5}AlSSe$	Ordering I	Al_S
$Cs_{0.5}Cu_{0.5}AlS_2$	Ordering I	Cs_S, Al_{Cu}
$Cs_{0.5}Cu_{0.5}AlTe_2$	Ordering I	Cs_{Al}, Cs_{Te}
$Cs_{0.5}Cu_{0.5}AlTe_2$	Ordering II	Te_{Cu}, Cu_{Te}, Al_i, V_{Al}, V_{Cu}
$Cs_{1.5}Ag_{0.5}MgSnS_2Se_2$	Ordering I	S_i, Cs_{Sn}, Cs_{Mg}, Ag_{Mg}, V_{Sn}
$CsAl_{0.5}Ga_{0.5}Se_2$	Ordering I	V_{Se}, Cs_i, Se_i, Ga_{Al}

Continued on next page

Table S3 – continued from previous page

Compound	**Ordering**	**Defects Considered**
$CsAlSeTe$	Ordering II	Al_{Te}
$CsAlSe_2$	Ordering I	V_{Cs}, Al_i
$CsAlSe_2$	Ordering II	V_{Se}
$CsAlTe_2$	Ordering I	Cs_i, Te_{Cs}, Cs_{Al}
$CsGaS_2$	Ordering I	V_S
$CsInS_2$	Ordering I	S_{Cs}
$Cs_2MgSnSe_4$	Ordering I	Mg_i, Mg_{Se}
$Cu_{0.5}Ag_{0.5}Al_{0.5}In_{0.5}SSe$	Ordering I	Al_S, S_{Al}, Cu_{Al}, In_{Se}, Al_{In}
$Cu_{0.5}Ag_{0.5}Al_{0.5}In_{0.5}SSe$	Ordering II	V_{Al}, Cu_{Al}, S_{In}, Se_{In}, In_{Ag}
$Cu_{0.5}Ag_{0.5}Al_{0.5}In_{0.5}STe$	Ordering I	V_{Al}, Al_S, S_{Cu}, Cu_{Al}
$Cu_{0.5}Ag_{0.5}Al_{0.5}In_{0.5}S_2$	Ordering I	Ag_{Cu}, In_{Al}
$Cu_{0.5}Ag_{0.5}Al_{0.5}In_{0.5}S_2$	Ordering II	S_{Cu}, S_{In}, S_i, Cu_{Al}
$Cu_{0.5}Ag_{0.5}Al_{0.5}In_{0.5}Se_2$	Ordering II	Se_{Ag}, V_{In}, Se_i, Al_{Se}
$Cu_{0.5}Ag_{0.5}AlSTe$	Ordering I	Ag_{Te}, V_{Te}, Ag_{Cu}, V_S, S_{Te}, Te_i
$Cu_{0.5}Ag_{0.5}AlSTe$	Ordering II	S_{Al}, Al_i
$Cu_{0.5}Ag_{0.5}AlS_2$	Ordering I	V_{Ag}, Ag_{Al}, V_{Al}
$Cu_{0.5}Ag_{0.5}AlS_2$	Ordering II	Ag_{Al}, Ag_i, Ag_S, V_{Cu}, S_{Ag}
$Cu_{0.5}Ag_{0.5}AlSeTe$	Ordering I	Al_{Se}, Cu_{Al}, V_{Te}
$Cu_{0.5}Ag_{0.5}AlSeTe$	Ordering II	Cu_{Te}, Te_{Se}, Te_i, V_{Al}, Ag_{Te}, Al_{Ag}

Continued on next page

Table S3 – continued from previous page

Compound	**Ordering**	**Defects Considered**
$Cu_{0.5}Ag_{0.5}AlSe_2$	Ordering I	V_{Se}, Cu_i, Cu_{Al}
$Cu_{0.5}Ag_{0.5}AlSe_2$	Ordering II	Se_{Cu}, Cu_{Se}, Cu_{Al}, Cu_i, V_{Cu}, Se_i
$Cu_{0.5}Ag_{0.5}AlTe_2$	Ordering I	Ag_{Te}, Al_{Ag}
$Cu_{0.5}Ag_{0.5}AlTe_2$	Ordering II	Te_{Ag}
$Cu_{0.5}Ag_{0.5}Ga_{0.5}In_{0.5}S_2$	Ordering I	S_{In}
$Cu_{0.5}Ag_{0.5}Ga_{0.5}In_{0.5}S_2$	Ordering II	Ga_S, Cu_{Ga}
$Cu_{0.5}Ag_{0.5}Ga_{0.5}In_{0.5}Se_2$	Ordering I	Ag_{Ga}, Ag_{Cu}, V_{Cu}, Ag_i
$Cu_{0.5}Ag_{0.5}Ga_{0.5}In_{0.5}Se_2$	Ordering II	Ag_{Ga}, Ag_i, Ga_i, Ga_{Cu}
$Cu_{0.5}Ag_{0.5}GaS_2$	Ordering I	Ag_{Ga}, S_{Cu}, Cu_{Ga}, Cu_{Ag}
$Cu_{0.5}Ag_{0.5}GaS_2$	Ordering II	Ag_S, Cu_{Ga}
$Cu_{0.5}Ag_{0.5}GaSe_2$	Ordering I	V_{Ag}, Se_{Ga}
$Cu_{0.5}Ag_{0.5}GaSe_2$	Ordering II	Cu_{Se}, Cu_{Ag}
$Cu_{0.5}Ag_{0.5}InS_2$	Ordering I	In_i, Cu_S
$Cu_{0.5}Ag_{0.5}InS_2$	Ordering II	Ag_{Cu}
$Cu_{0.5}Ag_{1.5}Zn_{0.5}Cd_{0.5}GeS_3Te$	Ordering I	Cd_{Zn}, Te_{Ge}, Te_S, Ge_{Ag}, Ge_{Te}, Zn_{Ag}, V_{Cd}, Ge_{Cd}, V_{Ag}, Cu_{Ag}, Ge_{Zn}, Cd_{Te}, S_{Cd}
$Cu_{1.5}Ag_{0.5}BaSnS_4$	Ordering I	Ag_i, Ag_S, S_{Cu}, Ba_{Sn}, Ba_S
$Cu_{1.5}Ag_{0.5}BaSnS_4$	Ordering II	V_{Ag}, Cu_{Ag}, Cu_{Ba}
$CuAl_{0.5}Ga_{0.5}S_2$	Ordering I	V_{Al}, Ga_{Al}, S_i

Continued on next page

Table S3 – continued from previous page

Compound	**Ordering**	**Defects Considered**
$CuAl_{0.5}Ga_{0.5}Te_2$	Ordering I	Ga_{Te}, Al_{Te}, V_{Cu}, V_{Al}
$CuAl_{0.5}In_{0.5}S_2$	Ordering I	S_{Cu}, S_{In}, In_{Cu}
$CuAl_{0.5}In_{0.5}S_2$	Ordering II	In_{Cu}
$CuAl_{0.5}In_{0.5}Se_2$	Ordering I	V_{Cu}, Se_{Al}
$CuAl_{0.5}In_{0.5}Se_2$	Ordering II	V_{Se}
CuAlSTe	Ordering I	Al_{Cu}
CuAlSTe	Ordering II	S_{Al}, Te_S, V_S
$CuAlS_2$	Ordering I	Cu_i, V_{Cu}
$CuAlS_2$	Ordering II	Al_i, Al_{Cu}
CuAlSeTe	Ordering I	Al_{Cu}, Cu_i, Te_{Al}
CuAlSeTe	Ordering II	Te_{Se}
$CuAlSe_2$	Ordering I	Cu_{Al}, Al_{Se}
$CuAlSe_2$	Ordering II	Se_i, Se_{Cu}, V_{Se}
$CuAlTe_2$	Ordering I	Cu_{Al}
$CuAlTe_2$	Ordering II	Te_{Cu}, Al_{Cu}, V_{Cu}
$CuGa_{0.5}In_{0.5}S_2$	Ordering I	V_{Cu}, V_{Ga}, S_{Ga}, V_S
$CuGa_{0.5}In_{0.5}S_2$	Ordering II	In_S, Cu_i
$CuGa_{0.5}In_{0.5}Se_2$	Ordering II	Se_{Cu}, In_{Se}
CuGaSSe	Ordering II	Cu_{Ga}, V_{Cu}

Continued on next page

Table S3 – continued from previous page

Compound	**Ordering**	**Defects Considered**
CuGaSTe	Ordering I	Ga_i, Cu_S, Cu_i, V_{Te}
$CuGaS_2$	Ordering I	Cu_{Ga}, Ga_S
$CuGaS_2$	Ordering II	V_S
CuGaSeTe	Ordering I	Te_i, Ga_{Te}
CuGaSeTe	Ordering II	Se_{Cu}, Cu_{Te}, Te_{Ga}, Ga_{Se}, V_{Cu}
$CuGaSe_2$	Ordering I	Se_{Cu}
CuInSSe	Ordering II	S_{Se}, Se_{Cu}
$CuInS_2$	Ordering I	Cu_i
$CuInS_2$	Ordering II	In_{Cu}
$CuInSe_2$	Ordering I	Se_{Cu}
$CuInSe_2$	Ordering II	Cu_{In}
Cu_2BaGeS_4	Ordering I	S_i
$Cu_2BaSn_{0.25}Zr_{0.75}S_4$	Ordering II	Ba_S, Zr_{Sn}, Ba_{Sn}, Cu_S
$Cu_2BaSn_{0.5}Zr_{0.5}S_4$	Ordering II	V_{Sn}, S_{Sn}
$Cu_2BaSn_{0.75}Zr_{0.25}S_4$	Ordering II	V_{Cu}, Zr_{Ba}, Cu_S, Ba_{Sn}
$Cu_2BaZrS_2Se_2$	Ordering II	Zr_{Se}, Zr_{Ba}, Cu_{Zr}
Cu_2BaZrS_4	Ordering I	S_{Zr}, S_{Cu}
Cu_2BaZrS_4	Ordering II	Zr_{Ba}, V_{Ba}, S_i
$Cu_2BaZrSe_4$	Ordering II	Ba_{Zr}, Ba_{Cu}

Continued on next page

Table S3 – continued from previous page

Compound	**Ordering**	**Defects Considered**
Cu_2CaGeS_4	Ordering II	S_{Cu}, V_S, S_i
$Cu_2CaGeSe_4$	Ordering II	Cu_{Ge}, Ca_{Ge}
Cu_2CaSnS_4	Ordering II	V_{Ca}, Cu_S
$Cu_2CdGeS_2Te_2$	Ordering II	Te_S, V_{Cd}, Cu_S, V_S
Cu_2CdGeS_4	Ordering II	V_S
$Cu_2CdGeSe_4$	Ordering II	V_{Cd}
$Cu_2CdSnS_2Se_2$	Ordering I	S_{Se}, Sn_{Se}, Cd_i, Se_{Sn}, Se_{Cd}
$Cu_2CdSnS_2Se_2$	Ordering II	Cd_{Sn}, Cu_{Sn}
Cu_2CdSnS_4	Ordering I	S_{Sn}, Cu_i, Cu_{Cd}, S_{Cu}
$Cu_2CdSnSe_4$	Ordering I	V_{Cu}, Cd_{Sn}, Se_{Cd}, Sn_i
$Cu_2Mg_{0.5}Ca_{0.5}SnS_4$	Ordering I	Mg_{Cu}, V_{Sn}
$Cu_2Mg_{0.5}Ca_{0.5}SnS_4$	Ordering II	Mg_{Ca}, Ca_S, V_{Sn}
$Cu_2Mg_{0.5}Ca_{0.5}SnSe_4$	Ordering II	Cu_{Se}, Ca_{Cu}, Mg_{Cu}, Sn_{Cu}, Se_i
$Cu_2Mg_{0.5}Sr_{0.5}ZrSe_4$	Ordering I	Mg_{Cu}, Sr_{Cu}
$Cu_2Mg_{0.5}Sr_{0.5}ZrSe_4$	Ordering II	Mg_i, Sr_{Zr}, Mg_{Sr}
Cu_2MgGeS_4	Ordering I	S_{Mg}, Cu_{Mg}, Mg_i
Cu_2MgGeS_4	Ordering II	Cu_i, S_i, Mg_i, Ge_{Cu}, Mg_{Cu}
$Cu_2MgGeSe_4$	Ordering I	V_{Cu}, Cu_{Ge}, V_{Ge}, Se_{Ge}
$Cu_2MgGeTe_4$	Ordering II	Te_{Ge}, V_{Cu}

Continued on next page

Table S3 – continued from previous page

Compound	**Ordering**	**Defects Considered**
$Cu_2MgSnSSe_3$	Ordering I	S_i, Cu_{Se}, Mg_{Sn}, S_{Cu}, Mg_i, Se_{Cu}, Cu_{Sn}
$Cu_2MgSnSTe_3$	Ordering II	S_{Sn}, Mg_{Te}, Te_{Cu}, S_i, V_{Sn}, V_S
$Cu_2MgSnS_2Se_2$	Ordering I	V_S, S_{Sn}, Mg_{Se}, Cu_S
$Cu_2MgSnS_2Se_2$	Ordering II	Mg_S, S_{Sn}, Mg_i, V_S
Cu_2MgSnS_3Se	Ordering I	Cu_{Se}, Sn_i, V_S, Sn_{Cu}
Cu_2MgSnS_3Se	Ordering II	S_i, Cu_{Se}, Mg_S, Cu_S
Cu_2MgSnS_4	Ordering I	S_{Mg}, S_{Cu}
Cu_2MgSnS_4	Ordering II	V_{Cu}, S_{Cu}
$Cu_2MgSnSe_4$	Ordering I	Se_{Cu}, Se_{Sn}, Cu_i
$Cu_2MgSnSe_4$	Ordering II	Mg_{Cu}, Se_{Cu}, V_{Mg}
$Cu_2MgZrTe_4$	Ordering I	Cu_{Zr}
$Cu_2MgZrTe_4$	Ordering II	Mg_i, V_{Te}, Te_{Zr}, Mg_{Zr}
Cu_2SrGeS_4	Ordering I	Cu_S
Cu_2SrGeS_4	Ordering II	V_S, S_{Ge}, Ge_{Cu}, Cu_{Sr}, S_{Cu}
$Cu_2SrGeSe_4$	Ordering II	Se_{Cu}, Cu_i
Cu_2SrSnS_4	Ordering II	Sr_S
Cu_2ZnGeS_2SeTe	Ordering I	Te_i, S_{Ge}, Te_{Se}, Ge_{Se}, Te_{Zn}, Se_{Zn}, V_{Zn}, Cu_{Te}
Cu_2ZnGeS_4	Ordering I	Ge_S

Continued on next page

Table S3 – continued from previous page

Compound	**Ordering**	**Defects Considered**
$Cu_2ZnGeSe_4$	Ordering II	V_{Se}
$Cu_2ZnSn_{0.25}Zr_{0.75}S_2Se_2$	Ordering II	Se_{Zr}, S_{Zn}, Sn_{Zn}, S_{Se}
$Cu_2ZnSn_{0.25}Zr_{0.75}S_4$	Ordering II	V_{Zn}, S_{Zn}
$Cu_2ZnSn_{0.5}Zr_{0.5}S_2Se_2$	Ordering I	Sn_{Zr}, Se_{Zr}, V_S, Zr_{Cu}
$Cu_2ZnSn_{0.5}Zr_{0.5}S_2Se_2$	Ordering II	Zr_{Sn}, S_i, Zr_{Cu}, V_{Zr}
$Cu_2ZnSn_{0.5}Zr_{0.5}S_4$	Ordering I	S_{Zr}, V_{Cu}, Zn_{Sn}, V_{Sn}, V_{Zr}
$Cu_2ZnSn_{0.5}Zr_{0.5}S_4$	Ordering II	Zr_i, Zn_{Sn}, Zr_{Cu}
$Cu_2ZnSn_{0.5}Zr_{0.5}Se_4$	Ordering I	Se_{Sn}, V_{Sn}, Sn_{Cu}, V_{Se}, Cu_{Zn}, Sn_{Zn}
$Cu_2ZnSn_{0.5}Zr_{0.5}Se_4$	Ordering II	Se_{Zn}
$Cu_2ZnSn_{0.75}Zr_{0.25}S_2Se_2$	Ordering I	Zn_{Cu}, Zn_{Se}, V_{Cu}, S_{Zn}
$Cu_2ZnSn_{0.75}Zr_{0.25}S_4$	Ordering I	Cu_S, Zr_{Zn}
$Cu_2ZnSn_{0.75}Zr_{0.25}S_4$	Ordering II	Cu_i, Sn_{Zn}
$Cu_2ZnSn_{0.75}Zr_{0.25}Se_4$	Ordering I	Cu_{Zn}, V_{Zn}
$Cu_2ZnSn_{0.75}Zr_{0.25}Se_4$	Ordering II	Sn_{Zn}, Se_{Zr}
$Cu_2ZnSnS_2Se_2$	Ordering I	Zn_{Se}, Se_{Zn}, Cu_{Se}
$Cu_2ZnSnS_2Se_2$	Ordering II	S_{Se}, Se_{Sn}, V_{Sn}, Cu_i
Cu_2ZnSnS_4	Ordering I	Zn_S, Sn_S, S_{Zn}, Cu_{Zn}
Cu_2ZnSnS_4	Ordering II	Zn_{Sn}, Zn_{Cu}, Sn_{Cu}, V_{Cu}
$Cu_2ZnSnSe_4$	Ordering I	Cu_i, Sn_{Se}, Sn_{Cu}

Continued on next page

Table S3 – continued from previous page

Compound	**Ordering**	**Defects Considered**
$Cu_2ZnSnSe_4$	Ordering II	V_{Se}, Sn_{Se}
$Cu_2ZnZrS_2Se_2$	Ordering I	Se_i, Se_{Cu}
Cu_2ZnZrS_4	Ordering I	Cu_{Zn}
Cu_2ZnZrS_4	Ordering II	Zn_{Zr}, V_S, S_{Zn}, Zn_i, S_{Cu}, Zr_S
$Cu_2ZnZrSe_4$	Ordering I	Zr_{Se}
$Cu_2ZnZrSe_4$	Ordering II	V_{Se}, Se_{Zn}, Se_{Cu}
$K_{0.5}Ag_{0.5}Al_{0.5}Ga_{0.5}STe$	Ordering I	Te_S, S_{Al}, Ga_{Ag}
$K_{0.5}Ag_{0.5}Al_{0.5}In_{0.5}S_2$	Ordering I	S_{Al}, Al_S, Al_K
$K_{0.5}Ag_{0.5}AlSTe$	Ordering I	S_{Ag}, Ag_K, Al_i, Al_{Te}, S_{Te}
$K_{0.5}Ag_{0.5}AlSTe$	Ordering II	S_{Al}, V_S
$K_{0.5}Ag_{0.5}AlS_2$	Ordering I	Al_{Ag}
$K_{0.5}Ag_{0.5}AlSeTe$	Ordering I	K_{Te}, Al_{Te}, Al_{Ag}, Te_{Al}, V_K, Te_i, Te_{Se}, Se_{Te}
$K_{0.5}Ag_{0.5}AlSeTe$	Ordering II	Se_{Ag}
$K_{0.5}Ag_{0.5}AlSe_2$	Ordering I	Ag_{Al}
$K_{0.5}Ag_{0.5}AlSe_2$	Ordering II	V_K, V_{Ag}, V_{Se}
$K_{0.5}Ag_{0.5}AlTe_2$	Ordering I	K_i, Al_{Ag}, Te_K
$K_{0.5}Ag_{0.5}AlTe_2$	Ordering II	Te_K, Ag_i, V_{Al}
$K_{0.5}Ag_{0.5}Ga_{0.5}In_{0.5}SSe$	Ordering I	In_S, K_S, In_i, Ga_{Se}, Ag_{Se}, Se_{In}, S_{In}
$K_{0.5}Ag_{0.5}GaS_2$	Ordering I	Ag_S, V_S, S_K

Continued on next page

Table S3 – continued from previous page

Compound	Ordering	Defects Considered
$K_{0.5}Ag_{0.5}GaS_2$	Ordering II	S_{Ga}, K_{Ga}, V_K, K_i
$K_{0.5}Ag_{1.5}SrZrS_4$	Ordering I	Sr_i, Ag_i, Zr_K
$K_{0.5}Ag_{1.5}SrZrS_4$	Ordering II	S_{Sr}, Ag_S
$K_{0.5}Cs_{0.5}Al_{0.5}Ga_{0.5}STe$	Ordering I	Cs_K, V_K, S_K, Te_{Al}, Cs_{Te}, Te_K
$K_{0.5}Cs_{0.5}Al_{0.5}In_{0.5}SSe$	Ordering I	V_{Se}, Cs_{In}, K_i, S_{In}, S_{Se}
$K_{0.5}Cs_{0.5}Al_{0.5}In_{0.5}SSe$	Ordering II	K_i, K_{Al}, K_S, Cs_{Al}, Cs_i, V_{Se}, In_{Cs}
$K_{0.5}Cs_{0.5}AlSe_2$	Ordering I	K_i, Al_{Se}
$K_{0.5}Cs_{0.5}AlTe_2$	Ordering I	Al_{Te}
$K_{0.5}Cs_{0.5}AlTe_2$	Ordering II	Cs_K, K_i
$K_{0.5}CsAg_{0.5}MgGeSe_4$	Ordering I	V_{Cs}, Se_{Ge}, Cs_{Ag}, Ge_{Cs}, Mg_i
$K_{0.5}Cu_{0.5}AgCdGeS_4$	Ordering II	Cu_K, Cd_i, Cd_{Ag}, V_S, K_{Ge}
$K_{0.5}Cu_{0.5}AgMg_{0.5}Zn_{0.5}GeSe_4$	Ordering I	Ge_{Se}, Mg_{Zn}, Ge_{Cu}, Cu_{Mg}, Mg_K, Se_{Ag}
$K_{0.5}Cu_{0.5}AgMg_{0.5}Zn_{0.5}GeSe_4$	Ordering II	K_{Ag}, Se_{Ge}, Mg_K, Zn_{Cu}
$K_{0.5}Cu_{0.5}Al_{0.5}Ga_{0.5}SSe$	Ordering I	Al_S, Ga_i, Se_{Ga}, Ga_K, Al_{Se}
$K_{0.5}Cu_{0.5}Al_{0.5}Ga_{0.5}SSe$	Ordering II	V_S, Cu_{Se}, Al_{Ga}, Ga_K, S_{Ga}, Se_{Cu}
$K_{0.5}Cu_{0.5}Al_{0.5}Ga_{0.5}S_2$	Ordering II	Ga_{Al}, Cu_{Al}, K_{Al}
$K_{0.5}Cu_{0.5}Al_{0.5}Ga_{0.5}SeTe$	Ordering I	Ga_{Cu}, V_{Ga}, K_{Ga}, Te_{Se}, Te_{Ga}, Te_{Al}
$K_{0.5}Cu_{0.5}Al_{0.5}Ga_{0.5}Se_2$	Ordering I	K_{Se}, V_{Se}, Al_i, Al_{Ga}
$K_{0.5}Cu_{0.5}Al_{0.5}Ga_{0.5}Se_2$	Ordering II	K_{Se}, V_{Cu}, Se_{Cu}, Se_K, Ga_i, Se_{Al}

Continued on next page

Table S3 – continued from previous page

Compound	**Ordering**	**Defects Considered**
$K_{0.5}Cu_{0.5}Al_{0.5}In_{0.5}S_2$	Ordering I	K_{Al}, Al_{Cu}, In_K, In_{Cu}
$K_{0.5}Cu_{0.5}Al_{0.5}In_{0.5}S_2$	Ordering II	S_{Al}, Cu_S
$K_{0.5}Cu_{0.5}AlS_2$	Ordering I	Al_i, Al_S, K_S, S_K, K_{Cu}
$K_{0.5}Cu_{0.5}AlS_2$	Ordering II	K_S, S_i
$K_{0.5}Cu_{0.5}AlSe_2$	Ordering I	V_{Se}, V_K, V_{Cu}, K_{Se}, Se_{Cu}, V_{Al}, Al_{Se}
$K_{0.5}Cu_{0.5}AlSe_2$	Ordering II	K_{Cu}, V_{Al}, V_{Cu}
$K_{0.5}Cu_{0.5}AlTe_2$	Ordering I	Al_{Te}, Te_K, V_{Cu}
$K_{0.5}Cu_{0.5}AlTe_2$	Ordering II	Cu_{Te}, K_{Cu}, Te_K
$K_{0.5}Cu_{0.5}GaS_2$	Ordering I	Cu_i
$K_{0.5}Cu_{0.5}GaS_2$	Ordering II	V_{Cu}, Cu_K
$K_{0.5}Cu_{1.5}ZnGeS_4$	Ordering II	Zn_{Cu}, S_{Cu}
$K_{0.5}CuAg_{0.5}CdZrS_4$	Ordering I	Cd_K, K_i, Ag_S, V_{Cd}, Cu_{Zr}
$K_{0.5}CuAg_{0.5}Mg_{0.5}Ca_{0.5}SnS_4$	Ordering II	S_{Cu}, V_{Mg}, Mg_{Ca}, Ca_S, K_{Cu}, Ca_i, K_S, Cu_K, V_{Cu}
$K_{0.5}Rb_{0.5}AgMg_{0.5}Zn_{0.5}GeS_3Te$	Ordering I	V_K, Rb_i, V_{Rb}, Zn_S, Rb_S, Te_{Ge}, Ge_{Rb}, Mg_{Zn}, Ge_K, Mg_i, Ge_{Zn}, Zn_i
$K_{0.5}Rb_{0.5}AgMg_{0.5}Zn_{0.5}GeSe_3$	Ordering I	Zn_i, Rb_{Se}, Zn_K, Se_i, Te_K, V_K, Ge_i
$K_{0.5}Rb_{0.5}AgMgGeS_4$	Ordering I	Ag_i, S_{Mg}, S_{Ag}, Ge_K, Ag_K, Ge_i, K_S, Rb_i, Ge_{Mg}, K_{Mg}, V_{Rb}, K_i, Mg_{Rb}

Continued on next page

Table S3 – continued from previous page

Compound	Ordering	Defects Considered
$K_{0.5}Rb_{0.5}AgMgGeS_4$	Ordering II	V_{Rb}, V_{Ge}, Mg_K
$K_{0.5}Rb_{0.5}AgZnGeS_4$	Ordering I	S_{Zn}, Ge_S, Ag_{Ge}, Rb_{Zn}, K_{Ag}
$K_{0.5}Rb_{0.5}AgZnGeS_4$	Ordering II	Ag_S, Ag_i, Rb_{Ag}, S_{Rb}, K_{Ge}
$K_{0.5}Rb_{0.5}Al_{0.5}Ga_{0.5}Se_2$	Ordering II	Ga_i, Se_i, Se_{Ga}
$K_{0.5}Rb_{0.5}AlS_2$	Ordering I	S_i
$K_{0.5}Rb_{0.5}AlSeTe$	Ordering I	Al_K, Te_K, Al_{Se}, V_{Te}
$K_{0.5}Rb_{0.5}AlSeTe$	Ordering II	Rb_{Al}, K_{Al}, V_{Se}
$K_{0.5}Rb_{0.5}AlSe_2$	Ordering I	Al_{Se}
$K_{0.5}Rb_{0.5}AlSe_2$	Ordering II	Se_K, Al_{Rb}
$K_{0.5}Rb_{0.5}AlTe_2$	Ordering I	V_{Rb}, K_{Rb}, Al_{Rb}
$K_{0.5}Rb_{0.5}AlTe_2$	Ordering II	Rb_{Al}
$K_{0.5}Rb_{0.5}Cs_{0.5}Ag_{0.5}MgSnSe_4$	Ordering I	Sn_{Rb}, Mg_{Cs}, V_{Mg}, Rb_{Cs}, Rb_{Sn}, Cs_{Mg}, Rb_i, Sn_K, Cs_{Rb}, K_{Mg}, V_{Sn}, Ag_{Mg}, Se_{Sn}, Rb_{Mg}, Ag_{Sn}, Se_{Cs}
$K_{0.5}Rb_{0.5}Cs_{0.5}Ag_{0.5}MgZrS_4$	Ordering I	S_{Cs}, Rb_S, Mg_i, Ag_{Mg}, Rb_K, Cs_i, Rb_{Cs}
$K_{0.5}Rb_{0.5}Cs_{0.5}Ag_{0.5}MgZrS_4$	Ordering II	K_S, S_{Ag}, Ag_{Rb}, K_{Mg}, Rb_i, K_i, V_S, Ag_K, S_{Mg}, V_{Mg}, Zr_S
$K_{0.5}Rb_{0.5}Cs_{0.5}Ag_{0.5}MgZrSe_4$	Ordering I	Rb_K, Zr_{Cs}, V_{Zr}, Zr_{Mg}, Mg_{Zr}, Rb_{Se}
$K_{0.5}Rb_{0.5}Cs_{0.5}Ag_{0.5}MgZrSe_4$	Ordering II	V_{Se}, Se_{Cs}, Se_{Zr}, Cs_{Ag}, Rb_{Mg}, Rb_{Ag}, Ag_{Rb}

Continued on next page

Table S3 – continued from previous page

Compound	Ordering	Defects Considered
$K_{0.5}Rb_{0.5}Cs_{0.5}Ag_{0.5}ZnGeS_4$	Ordering I	V_{Ag}, Zn_i, Ge_{Ag}, Rb_i, Ag_{Zn}, Ge_S, Rb_S, Ag_{Ge}, V_{Cs}
$K_{0.5}Rb_{0.5}Cs_{0.5}Ag_{0.5}ZnGeS_4$	Ordering II	Rb_{Zn}, Ge_i, Ge_{Rb}, Ag_K, Zn_{Cs}, Cs_S
$K_{0.5}Rb_{0.5}CsZnZrS_4$	Ordering I	Zn_i, Cs_S, Rb_K, V_{Cs}, K_{Cs}, V_{Zr}, V_{Zn}, K_{Zn}
$K_{0.5}Rb_{0.5}Cu_{0.5}Ag_{0.5}MgGeS_4$	Ordering II	Mg_K, Ge_{Ag}, Cu_{Mg}, Cu_{Ag}, V_K, Mg_{Rb}, Rb_i, K_S
$K_{0.5}Rb_{0.5}CuZnZrS_4$	Ordering I	V_{Rb}, Rb_{Cu}, Cu_S, Rb_{Zr}, Zn_{Cu}
$K_{0.5}Rb_{0.5}CuZnZrS_4$	Ordering II	V_{Cu}, Rb_i, V_{Rb}, S_{Rb}, K_i
$K_{0.5}Rb_{0.5}GaSe_2$	Ordering I	Ga_K, Rb_K

Linear Correlation between Elemental Features and Target Properties

Each compound in the dataset is represented by a 50-dimensional feature vector composed of 48 elemental descriptors and 2 ordering indicators. The elemental descriptors are constructed from 12 fundamental elemental properties evaluated for the A, B, C, and X crystallographic sites using composition-weighted averages. Two additional binary features encode the cation ordering type (**Table S4**). Using this representation, we computed Pearson correlation coefficients between each descriptor and the target properties $\varepsilon_{optical}$, ΔH_{decomp}, E_{gap}, and SLME. For clarity, only the most strongly correlated descriptors are discussed here. The dielectric constant $\varepsilon_{optical}$ is dominated by X-site properties, particularly the X-site heat of fusion, melting point, ionic radius, electronegativity, and heat of vaporization, confirming the central role of anion chemistry. In contrast, ΔH_{decomp} is primarily governed by C-site

properties, with the C-site boiling point, heat of vaporization, electronegativity, melting point, and ionic radius showing the strongest correlations. The bandgap E_{gap} shows strong negative correlations with several A-site thermochemical descriptors (heat of vaporization, boiling point, heat of fusion, and melting point) and with the X-site atomic weight, reflecting the systematic reduction of E_{gap} with heavier and more weakly bound ions. Finally, SLME correlates most strongly with A-site properties, particularly the A-site ionization energy, electronegativity, melting point, heat of vaporization, and heat of fusion, while the A-site ionic radius shows a notable negative correlation. Overall, these trends reveal a clear site-wise chemical control of $\varepsilon_{optical}$ response, stability, E_{gap}, and photovoltaic efficiency, motivating the subsequent ML modeling.

Table S4: Full correlation table for Dielectric Constant, Decomposition Energy, Bandgap, and SLME.

Dielectric Const		**Decomp**		**Bandgap**		**SLME**	
Feature	Corr	Feature	Corr	Feature	Corr	Feature	Corr
X_{Heat_fusion}	0.509	C_{BP}	0.596	A_{Heat_vap}	-0.492	A_{Ion_Energy}	0.359
X_{MP}	0.507	C_{Heat_vap}	0.590	A_{BP}	-0.492	$A_{Electronegativity}$	0.359
X_{Ion_rad}	0.507	$C_{Electronegativity}$	-0.529	A_{Heat_fusion}	-0.491	A_{MP}	0.358
$X_{Electronegativity}$	-0.501	C_{MP}	0.526	A_{MP}	-0.489	A_{Heat_vap}	0.357
X_{Heat_vap}	0.499	C_{Ion_rad}	0.484	X_{At_wt}	-0.482	A_{Heat_fusion}	0.356
A_{Heat_vap}	0.496	C_{Period}	0.370	X_{Period}	-0.482	A_{BP}	0.356
A_{BP}	0.495	A_{Ion_rad}	0.330	X_{At_num}	-0.482	A_{Elec_Aff}	0.356
X_{BP}	0.493	C_{Elec_Aff}	-0.314	X_{Ion_Energy}	0.481	$A_{Density}$	0.352

Continued on next page

Table S4 – continued from previous page

Dielectric Const		Decomp		Bandgap		SLME	
Feature	Corr	Feature	Corr	Feature	Corr	Feature	Corr
A_{Heat_fusion}	0.493	A_{Heat_vap}	-0.303	X_{BP}	-0.481	A_{Ion_rad}	-0.311
X_{Ion_Energy}	-0.492	A_{BP}	-0.302	$A_{Electronegativity}$	-0.481	$X_{Density}$	0.276
A_{MP}	0.490	A_{Ion_Energy}	-0.297	X_{Elec_Aff}	0.481	X_{Elec_Aff}	-0.267
X_{At_wt}	0.485	A_{Heat_fusion}	-0.295	A_{Ion_Energy}	-0.480	X_{Period}	0.263
A_{Ion_Energy}	0.484	A_{MP}	-0.291	X_{Heat_vap}	-0.479	X_{At_num}	0.263
X_{Period}	0.483	$A_{Electronegativity}$	-0.280	A_{Elec_Aff}	-0.474	X_{At_wt}	0.262
X_{At_num}	0.483	A_{Elec_Aff}	-0.270	$X_{Density}$	-0.472	X_{Ion_Energy}	-0.257
$A_{Electronegativity}$	0.480	$A_{Density}$	-0.249	X_{Ion_rad}	-0.471	X_{BP}	0.256
X_{Elec_Aff}	-0.476	X_{Period}	0.241	X_{MP}	-0.471	X_{Heat_vap}	0.250
A_{Elec_Aff}	0.473	X_{At_num}	0.241	$A_{Density}$	-0.469	X_{Ion_rad}	0.235
$A_{Density}$	0.460	X_{At_wt}	0.241	X_{Heat_fusion}	-0.461	X_{MP}	0.234
$X_{Density}$	0.446	X_{Elec_Aff}	-0.241	A_{Ion_rad}	0.427	X_{Heat_fusion}	0.222
A_{Ion_rad}	-0.445	X_{Ion_Energy}	-0.241	$X_{Electronegativity}$	0.425	$X_{Electronegativity}$	-0.184
$B_{Electronegativity}$	0.215	X_{BP}	0.241	B_{Ion_Energy}	-0.303	B_{Ion_Energy}	0.157
B_{MP}	-0.206	X_{Heat_vap}	0.240	$B_{Electronegativity}$	-0.290	B_{BP}	-0.143
B_{Ion_Energy}	0.204	$X_{Density}$	0.238	B_{MP}	0.271	$B_{Electronegativity}$	0.127
$B_{Density}$	0.202	$B_{Electronegativity}$	-0.235	$B_{Density}$	-0.265	Ordering II	0.107

Continued on next page

Table S4 – continued from previous page

Dielectric Const		Decomp		Bandgap		SLME	
Feature	Corr	Feature	Corr	Feature	Corr	Feature	Corr
B_{Elec_Aff}	0.151	X_{Ion_rad}	0.235	$C_{Electronegativity}$	-0.261	Ordering I	-0.107
B_{Heat_fusion}	-0.145	X_{MP}	0.235	C_{Heat_vap}	0.247	B_{Ion_rad}	-0.105
B_{Ion_rad}	-0.131	B_{Ion_rad}	0.232	C_{MP}	0.247	B_{MP}	-0.101
B_{BP}	-0.126	X_{Heat_fusion}	0.230	C_{BP}	0.242	$B_{Density}$	0.095
A_{Period}	-0.123	B_{MP}	0.221	C_{Elec_Aff}	-0.225	B_{Heat_vap}	-0.095
C_{MP}	-0.091	B_{Heat_vap}	-0.213	B_{BP}	0.217	C_{At_wt}	0.086
C_{Heat_vap}	-0.087	$X_{Electronegativity}$	-0.211	B_{Heat_fusion}	0.198	C_{At_num}	0.084
C_{BP}	-0.087	A_{Period}	0.194	B_{Ion_rad}	0.190	$C_{Density}$	0.075
$C_{Electronegativity}$	0.084	$C_{Density}$	0.185	Ordering I	0.169	B_{Heat_fusion}	-0.070
B_{Heat_vap}	-0.063	Ordering II	0.170	Ordering II	-0.169	C_{Elec_Aff}	0.066
C_{Elec_Aff}	0.058	Ordering I	-0.170	B_{Elec_Aff}	-0.162	B_{Period}	-0.063
C_{Ion_rad}	-0.044	B_{Elec_Aff}	-0.141	C_{Ion_rad}	0.151	A_{At_num}	0.063
C_{At_wt}	0.042	C_{Ion_Energy}	-0.128	C_{Ion_Energy}	-0.140	A_{Period}	-0.056
C_{At_num}	0.039	B_{BP}	-0.121	B_{Heat_vap}	0.131	C_{MP}	-0.056
C_{Heat_fusion}	-0.038	A_{At_wt}	0.120	C_{At_wt}	-0.119	$C_{Electronegativity}$	0.053
B_{At_num}	0.037	C_{At_num}	0.115	C_{At_num}	-0.110	C_{Period}	0.053
$C_{Density}$	0.033	B_{Period}	0.114	A_{At_num}	-0.087	A_{At_wt}	0.049

Continued on next page

Table S4 – continued from previous page

Dielectric Const		**Decomp**		**Bandgap**		**SLME**	
Feature	Corr	Feature	Corr	Feature	Corr	Feature	Corr
B_{At_wt}	0.030	B_{Heat_fusion}	0.110	$C_{Density}$	-0.080	C_{Heat_vap}	-0.044
C_{Ion_Energy}	0.026	A_{At_num}	0.108	C_{Heat_fusion}	0.070	C_{Ion_Energy}	0.041
A_{At_num}	0.023	C_{Heat_fusion}	0.093	A_{At_wt}	-0.069	C_{BP}	-0.040
Ordering II	-0.019	$B_{Density}$	-0.093	A_{Period}	0.065	C_{Heat_fusion}	-0.040
Ordering I	0.019	C_{At_wt}	0.091	B_{Period}	0.048	B_{At_wt}	-0.030
B_{Period}	-0.018	B_{At_num}	0.051	B_{At_num}	-0.030	B_{At_num}	-0.027
C_{Period}	-0.005	B_{At_wt}	0.049	C_{Period}	0.021	B_{Elec_Aff}	0.014
A_{At_wt}	0.003	B_{Ion_Energy}	-0.036	B_{At_wt}	-0.021	C_{Ion_rad}	0.004